Journal of Molecular Catalysis A: Chemical 300 (2009) 48–58

Contents lists available at ScienceDirect

Journal of Molecular Catalysis A: Chemical

journal homepage: www.elsevier.com/locate/molcata

Cross-linked poly-vinyl polymers *versus* polyureas as designed supports for catalytically active M^0 nanoclusters
Part II. Pd^0/cross-linked poly-vinyl polymers *versus* Pd^0/EnCat^{TM}30NP in mild hydrogenation reactions

P. Centomo[a], M. Zecca[a], M. Kralik[b], D. Gasparovicova[c], K. Jerabek[d], P. Canton[e], B. Corain[a,f,*]

[a] *Dipartimento di Scienze Chimiche, Università degli Studi di Padova, Via Marzolo 1, 35131 Padova, Italy*
[b] *VUCHT j.s.c., Nobelova 34, SK-836 03 Bratislava, Slovak Republic*
[c] *Department of Organic Technology, Slovak University of Technology, Radlinskeho 9, SK-812 37 Bratislava, Slovak Republic*
[d] *Institute of Chemical Processes Fundamentals, Academy of Sciences of the Czech Republic, Rozvojova 135, 165 02 Praha 6, Suchdol, Czech Republic*
[e] *Dipartimento di Chimica Fisica, Università di Venezia, via Torino 155/b, 30170 Venezia-Mestre, Italy*
[f] *Istituto di Scienze e Tecnologie Molecolari, C.N.R., Sezione di Padova, Via Marzolo 1, 35131 Padova, Italy*

ARTICLE INFO

Article history:
Received 16 May 2008
Received in revised form 6 October 2008
Accepted 13 October 2008
Available online 5 November 2008

Keywords:
Cross-linked functional polymer
Support
Palladium(0) catalyst
Hydrogenation
Alkene
Nitroaromatics

ABSTRACT

Innovative Pd^0 heterogeneous catalysts were prepared upon using cross-linked, gel-type, functional acrylic polymers as the supports, along a simple route in use in our laboratories since long. The supports were obtained by polyaddition co-polymerization of *N*,*N*-dimethylacrylamide with either 2-acrylamido-2-methylpropane sulfonic acid, methacrylic acid or 4-vinylpyridine, and ethylene glycoldimethacrylate (cross-linker). The performance of these catalysts in the hydrogenation of cyclohexene, *trans*-methylcinnamate and 4-chloro-2-nitroanisole was compared with that of commercial Pd^0/EnCat 30NP, produced by Reaxa. One of the catalysts (sulfonic resin as the support) behaved very well as far as activity, stability and selectivity are concerned. These results suggest that heterogeneous metal catalysts supported on polyaddition resins could be developed to become interesting materials for technical applications.

1. Introduction

Until the beginning of this decade catalysts of the type M^0/CFP (M = metal center; CFP = cross-linked functional polymer) did not experience a considerable popularity [1]. The manufacture of bulk chemicals (commodities and semi-commodities) has been the traditional field of application of heterogeneous catalysts throughout the XX century. Bulk chemical production usually requires drastic reaction conditions, which are not compatible with moderate thermal stability of organic polymers. However, incessantly growing environmental concern is boosting a restless quest of "greener" ways to synthesize and produce fine and specialty chemicals. In fact, the replacement of stoichiometric syntheses with catalyzed ones is now considered a corner stone of modern industrial production of fine chemicals [2].

Catalysts based on CFPs offer *a priori* a degree of behavioural flexibility (*vide infra*) that is practically unknown for similar reactive materials based on inorganic supports. The reason for that is essentially the unique designability of the chemical, physico-chemical and structural properties of CFPs [3,4], which is quite superior of that of the inorganic supports [3]. In fact, the possibility of tuning the structural and chemical properties of the material as a function of the target application is certainly one of the most attractive features of these catalysts, as shown by the paradigmatic case of the bifunctional catalyst employed in the industrial synthesis of methylisobutylketone from acetone and hydrogen, i.e. Pd^0 supported on acidic sulfonated PS-DVB [5].

In common with heterogeneous metal catalysts M^0/CFP catalysts (i) can be easily separated from the reaction mixture; (ii) are generally not pyrophoric; (iii) are generally stable enough to be recycled.

In fact, molecular engineering of organic polymers, as compared with inorganic materials, is still at a superior level and the availability of materials featured by a large spectrum of chemical functionalization and physico-chemical properties can be still

* Corresponding author at: Dipartimento di Scienze Chimiche, Università degli Studi di Padova, Via Marzolo 1, 35131 Padova, Italy.
E-mail address: benedetto.corain@unipd.it (B. Corain).

1381-1169/$ – see front matter © 2008 Elsevier B.V. All rights reserved.
doi:10.1016/j.molcata.2008.10.039

Ⓟ-F_i + ML_n → Ⓟ-F_i-ML_n (1)

Ⓟ-F_i-ML_n+ reductant → M^0/Ⓟ-F_i (2)

M = metal centre; Ⓟ = CFP; Fi = F1, F2, …, Fn = desired functional group

Scheme 1. Synthesis routes to CFP-supported metal catalysts. The presence of F_i functionalities can make Ⓟ-F_i-ML_n and M^0/Ⓟ-F_i catalysts multi-functional in nature.

considered a unique feature of CFPs. This allows a straightforward approach to multi-functionality (Scheme 1) by design, which, for example, makes possible to perform consecutive reactions in a one-pot fashion (*vide infra*), as it is the case of the above-mentioned industrial synthesis of methylisobutylketone from acetone and molecular hydrogen [4]. Finally, the polymer framework of the CFP can act as a template, which allows controlling the final size of the supported metal nanoclusters during the preparation of M^0/CFP catalysts (Template Controlled Synthesis) [6]. For all these reasons, the interest in this kind of supported metal catalysts has been steadily growing for about 10 years [7], as it is demonstrated by the recent papers by Baiker's and Hölderich's groups, respectively on the industrially important selective one-pot synthesis of 2-ethyhexanal from crotonaldehyde in $scCO_2$, the hydroxylation of benzene to phenol with O_2 in the presence of H_2 and the synthesis of an analgesic with complex molecular structure [8,9].

The probably most general synthetic approach to M^0/CFP catalysts is illustrated in Scheme 1 and has been widely applied in our laboratories since long [7].

It is based on the uptake of a metal precursor by the CFP from a solution, assisted by the interaction of metal centers with the functional groups of the CFP (ion-exchange or metal coordination), followed by the reduction of the immobilized precursor to the zerovalent metal nanoclusters. Recently, a different approach, the microencapsulation of palladium acetate into a polyurea (Scheme 2) insoluble matrix and the reduction thereof, has been applied to the preparation of the so-called Pd^0/EnCat^{TM} commercial catalyst [10].

The Pd^0/EnCat catalysts are produced in different forms. Some of them differ in the size of palladium nanoclusters, depending on the way of reduction of palladium(II) in the precursor. Whereas reduction with dihydrogen yields nanoclusters of ca. 5 nm, when formic acid is employed as the reducing agent the obtained catalysts have much smaller nanoparticles (ca. 2 nm) and are labelled with the NP suffix [10]. The investigation on the nanometer scale morphology of two polyurea supports, i.e. EnCat 30 and EnCat 40 and of two related palladium catalysts Pd^0/EnCat 30NP and Pd^{II}/EnCat 30 from our laboratories is reported in Parts I and III of this series [11]. Whereas EnCat 30 and EnCat 40 result to be poorly accessible materials [11a], Pd^{II}/EnCat 30 and Pd^0/EnCat 30NP show a much different morphology, which makes them remarkably accessible to reagents and products of substantial size [11b].

We illustrate herein the synthesis and characterization at the nanometer scale of three cross-linked functional acrylic polymers (CFAP) (Scheme 3), their transformation into Pd^0/CFAP catalysts and the comparison between their performance with that of Pd^0/EnCat 30NP in the hydrogenation, under very mild conditions, of cyclohexene, some functional alkenes and 4-nitro-2-chloroanisole.

2. Experimental

2.1. Materials and apparatus

Chemicals were of reagent grade and were used as received. Pd^0/EnCat 30NP was supplied by Reaxa Ltd.

Elemental analyses were carried out with a Carlo Erba Fisons EA1108CHNS-O analyzer. XRMA samples were cut upon using a Buhehler Petri-Thin apparatus and covered by a carbon layer with MED 010 BALZERS apparatus. The analysis was carried out with an ESEM Philips XL30 apparatus. TEM analysis was carried out with a JEM 3010 (JEOL) electron microscope operating at 300 kV, with the Lens parameters Cs = 0.6 mm and Cc = 1.3 mm, giving a point resolution of 0.17 nm at Scherzer defocus. Thermogravimetric analysis was carried out with a SDT2960 thermobalance (TA Instruments) coupled with a Nicolet Nexus FT-IR apparatus, equipped with a Nicolet TGA interface. TG curves were recorded under a working N_2 flux equal to 70 cm^3 min^{-1}, with a heating rate equal to 20 °C min^{-1}. The measurements were carried out on about 10 mg of sample in an open alumina pan. ISEC characterization was performed upon employing D_2O, sugars and polydextranes as standard solutes in THF-swollen materials as described elsewhere [12]. GC–MS was performed on a Varian Saturn 2100T with GC 3900 containing a CP-Sil 8CB low bleed/MS 30 m × 0.25 mm, 0.25 μm column.

2.2. Synthesis of the supports

CFAP supports were synthesized starting from *N*,*N*-dimethylacrylamide (DMAA) and one out of the following

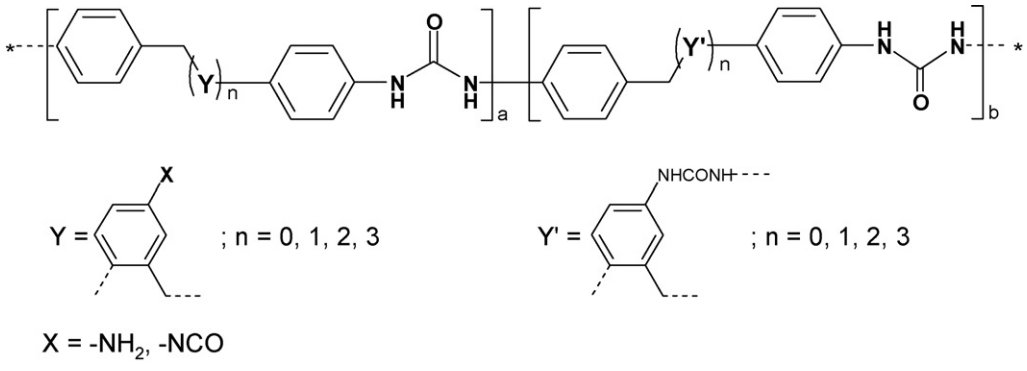

Scheme 2. Sketch of the polyurea insoluble matrix of EnCat^{TM} catalysts.

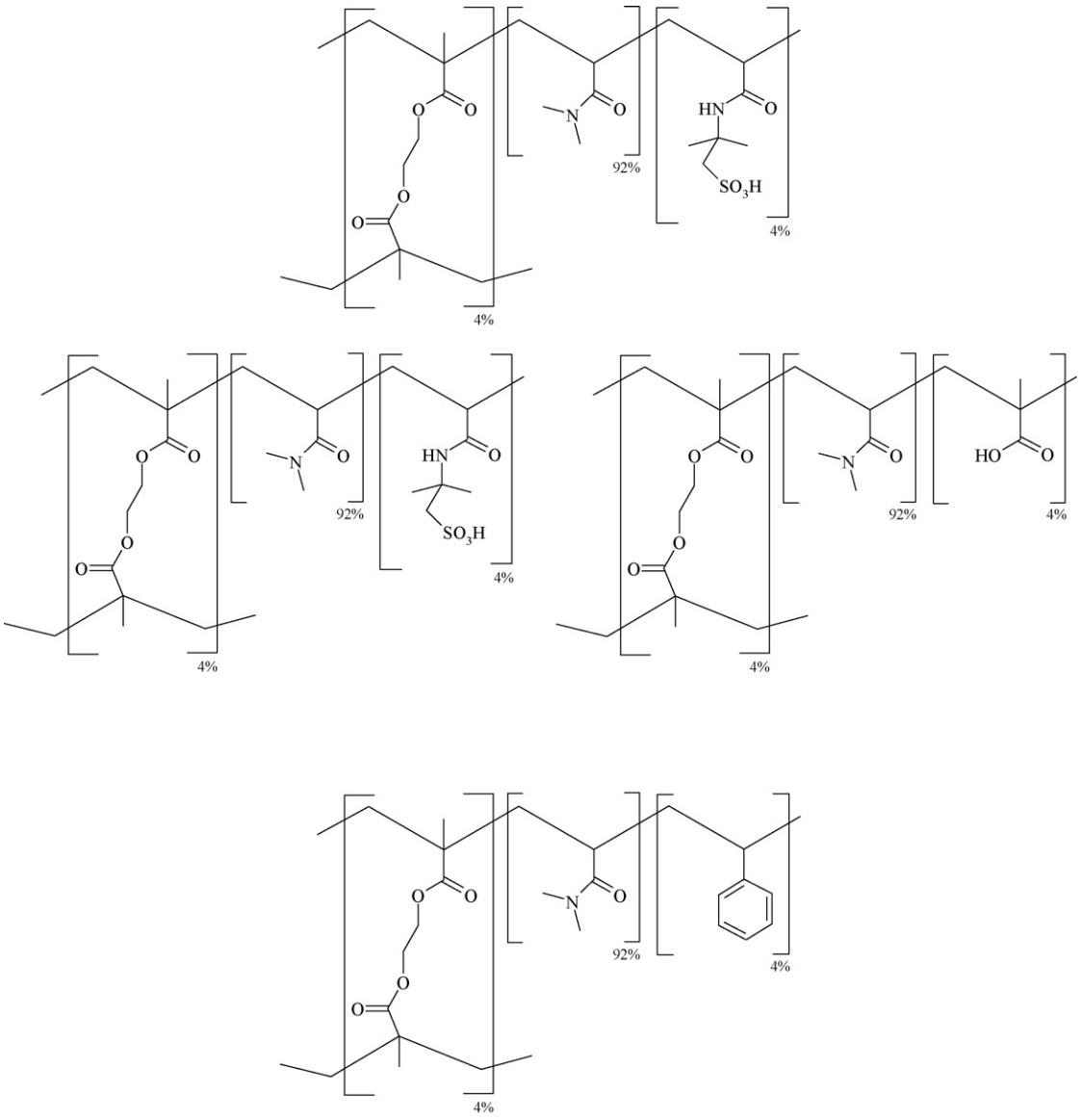

Scheme 3. Sketch of the primary structure of CFAP supports PSA, PMA, PVIP.

co-monomers: 2-acrylamido-2-methylpropane sulfonic acid (AMPSA), methacrylic acid (MA), 4-vinylpyridine (4-VIP). The cross-linking agent was ethylene glycol dimethacrylate (EDMA with nominal cross-linking degree equal to 4% mol/mol). The composition of the polymerization mixture was set to give the sulfonic (PSA), carboxylic (PMA) and pyridyl (PVIP) CFAP materials with ca. 0.4 mmol g^{-1} of functional group (Table 1).

The homogeneous liquid mixtures of the co-monomers and the cross-linker were prepared in pyrex cyclindical vials with screw-caps and de-aerated by bubbling N_2 to remove O_2. After closing the vials, the mixtures were irradiated with γ-rays from a ^{60}Co source up to a total dose of ca. 10 kGy. At the end, the CFAPs formed as cylindrical rods of the same internal size of the vials. After breaking the glass container, the rods were placed in pools of methanol (ca. 250 cm^3) and left under moderate stirring for 48 h. This treatment lead to de-colouration of the rods and to their extensive swelling. As the consequence of the latter, the polymer mass eventually broke apart in smaller pieces. After grinding (pestle and mortar) the recovered broken polymer samples, CFAPs were washed for further 48 h with methanol in a Soxhlet apparatus. Finally, they were recovered by filtration, dried over the filter for ca. 3 h at room temperature (membrane pump) and dried to constant weight at 60 °C in a vacuum oven. Polymerization yields were determined from the weights of the dry samples. Elemental analyses (C, H, N, S) are reported in Table 2.

Table 1
Composition of the polymerization mixtures[a] and polymerization yields.[b].

Support	DMAA	Functional co-monomer	EDMA	Polymerization yield (%)
PSA	8.60	0.78 (AMPSA)	0.75	98
PMA	8.90	0.34 (MA)	0.79	90
PVIP	8.93	0.42	0.78	97

[a] Amounts of co-monomers in grams.
[b] From the weight of dry recovered CFAPs.

The amount of acidic functional groups in PSA and PMA was 0.38 meq/g in both materials and was measured by acid–base titration as follows: an exactly weighed amount of CFAP (250 mg) was allowed to swell for a few hours in 2.5 cm^3 of boiled de-ionized water in a carefully stoppered Erlenmeyer flask. Then, 2.5 cm^3 of a

Table 2
Elemental analysis of CFAPs.[a].

Support	C	H	N	S
PSA	56.6 (58.63	8.9 (10.5)	11.7 (12.6)	1.3 (1.2)
PMA	59.1 (60.0)	9.0 (10.6)	11.6 (12.6)	–
PVIP	58.1 (60.9)	8.9 (10.7)	11.9 (13.1)	–

[a] %, w/w, theoretical values for 100% polymerization in parenthesis.

standard aqueous NaOH solution (0.11 M) were added to both the fully swollen CFAP and to 2.5 cm^3 of boiled de-ionized water (blank experiment). After 24 h of moderate magnetic stirring, the CFAP was separated by filtration and washed with three 1 cm^3 portions of de-ionized water. The amount of acidic functional groups was obtained as the difference between the amount of initially delivered NaOH and the amount of back-titrated NaOH in the recovered liquid (filtrate + washings), corrected with the amount of NaOH consumed in the blank experiment due to reaction with atmospheric CO_2.

2.3. Preparation of CFAP supported catalysts

The catalysts were prepared by palladiation of the CFAPs with $[Pd(NH_3)_4](NO_3)_2$, followed by reduction with $NaBH_4$. In a typical procedure the CFAP was let to fully swell in water (ca. 10 cm^3 per gram of dry material). Then a solution of the palladium complex (Table 3) in water (ca. 5 cm^3 per gram of dry material) was added to the suspension, which was gently mechanically swirled overnight. Only for PMA, the CFAP was directly added to the aqueous solution of $[Pd(NH_3)_4](NO_3)_2$. The metalated CFAP was separated upon filtration and washed over the filter with 3–4 portions of water (20 cm^3 each) and dried. The whole liquid phase (filtrate + washings) was recovered and analysed (ICP-AA) for unreacted palladium (Table 3).

The metalated CFAP was then swollen in deionized water (15–20 cm^3) and treated with $NaBH_4$ (0.25 g) dissolved in 5–10 cm^3 of water until the evolution of gas subsided. The solid was finally recovered upon filtration, washed with deionized water until neutral pH of the filtrate and dried at 60 °C at ca. 8 hPa up to constant weight.

2.4. ISEC characterization of CFAPs

D_2O, sugars, and polydextranes were employed as standard solutes in ISEC characterization of water-swollen resins. Details of the experimental procedure and data treatment were reported elsewhere [12].

2.5. Preparation of samples for XRMA analysis

Few milligrams of the samples were incorporated inside a drop of epoxy-resin (Araldite 2020 A/B) on the surface of a microscope slide. The resin was let to harden in an oven at 40 °C for 24 h. The upper part of the specimen was cut in order to show cross-sections of the incorporated particles. The surface was lapped with rubbing paper sheets soaked with an alcoholic suspension of diamond powder and fixed on rotating plates. A thin layer of carbon was finally deposited on the surface.

Table 3
Balance of palladium in the reaction of $[Pd(NH_3)_4](NO_3)_2$ with CFAPs.[a].

	Dry CFAP (g)	$[Pd(NH_3)_4](NO_3)_2$ (mg)[a]	Unreacted Pd (mg)	%Pd[b]
PSA	3.000	88 (31)	0.65	1.02
PMA	2.003	120 (43)	5.6	1.87
PVIP	1.192	66 (24)	18.6	0.45

[a] Weight of palladium in parentheses.
[b] Weight percentage in the dry metalated CFAP.

Table 4
Catalyst amounts in cyclohexene hydrogenation.

	%Pd (w/w) in the catalyst	Catalyst weight (mg)	Alkene/Pd (mol/mol)
Pd^0/NaPSA	1.02	191.5	327
Pd^0/NaPMA	1.87	191.5	178
Pd^0/PVIP	0.45	191.5	741
Pd^0/EnCat 30NP	4.26	47.9	313
Pd^0/Al_2O_3	0.99	191.5	337

2.6. Preparation of samples for TEM analysis

A few milligrams of the powder samples were mixed with high-purity isopropyl alcohol: the suspension was sonicated for 5 min in order to disrupt possible agglomerates. A 5 cm^3 droplet of suspension was transferred onto an amorphous carbon film, coating a 200 mesh copper grid (TAAB Laboratories Equipment Ltd.), and dried at room temperature, and then put into the microscope.

2.7. Catalytic hydrogenation of cyclohexene

The catalyst (ca. 2 mg of total palladium; see Table 4 for details) was introduced into a 15 cm^3 glass vessel and swollen in 10 cm^3 of methanol. After 1 h, the liquid was completely removed with a syringe and 6 cm^3 of 1 M solution of cyclohexene (alkene/Pd varied from 178 to 741 mol/mol) in methanol were poured onto the swollen catalyst.

The catalytic tests with hydrogenation of cyclohexene were carried out in a glass lined pressostatic reactor according to a procedure described previously [13]. To check for residual catalytic activity in the liquid phase after catalyst's separation (Maitlis or split test), a catalytic run was carried out up to virtually full conversion (less than 0.3 wt.% of unreacted cyclohexene). After careful settling of the solid, a portion of the liquid phase (2 cm^3) was removed and transferred into a clean glass reactor vessel, followed by the addition of 2 cm^3 of a cyclohexene solution in methanol (1 M). Finally the vessel was put inside the autoclave. To avoid possible deactivation of active species in the liquid phase (if any), these operations were carried out under nitrogen atmosphere. From this point on, the reaction was carried out in the same way as in straight catalytic runs.

2.8. Catalytic hydrogenation of trans-methylcinnamate

The catalyst was added to a solution of *trans*-methylcinnamate (0.5 mmol; Pd/alkene = 1/40, mol/mol, Pd^0/EnCat 30NP; 1/200, mol/mol, Pd^0/NaPSA) in methylated spirits (IMS, 5 cm^3). The reaction vessel was then flushed with hydrogen and stirred at room temperature. Aliquots of the reaction mixture were periodically removed and analysed by GC–MS (Table 5).

Table 5
Catalyst amounts in *trans*-methylcinnamate hydrogenation.

Catalyst	%Pd (w/w) in the catalyst	Catalyst weight (mg)	Alkene/Pd (mol/mol)
Pd^0/EnCat 30NP	4.26	59 (47% wet)	40
Pd^0/NaPSA	1.02	26.5	196

Table 6
Catalyst amounts in 4-chloro-2-nitroanisole hydrogenation.

Catalyst	%Pd (w/w) in the catalyst	Catalyst weight (mg)	Alkene/Pd (mol/mol)
Pd^0/EnCat 30NP	4.26	24 (47% wet)	100
Pd^0/NaPSA	1.02	53	98

2.9. Catalytic hydrogenation of 4-chloro-2-nitroanisole

The catalyst was added to a solution of 4-chloro-2-nitroanisole (0.5 mmol; Pd/nitroaromatic = 1/100, mol/mol) in methanol (5 cm^3). The reaction vessel was then flushed with hydrogen and stirred at room temperature. Aliquots of the reaction mixture were periodically removed and analysed by GC–MS (Table 6).

3. Results

3.1. Synthesis and characterization (TGA, ISEC) of CFAPs

PSA, PMA and PVIP (Scheme 3) were obtained as colourless, irregularly shaped particles in the 150–400 μm range. The action of γ-rays from ^{60}Co source lead, as expected from our long lasting experience [14], to polymerization yields near to 100%. The amount of functional groups in the acidic supports (PSA, sulfonic; PMA, carboxylic) is 0.38 mmol g^{-1} for both, close to the target value of 0.4 mmol g^{-1}. For PVIP the load of pyridyl groups was not determined, but in view of the high polymerization yield (almost quantitative) a functionalization degree close to the desired 0.4 mmol g^{-1} is expected. The elemental analyses are compatible with the expected composition of the materials, with a content of residual methanol around 8% (PSA, PMA), which was impossible to eliminate completely. The presence of residues of solvent within the polymer framework was confirmed by TG analysis of PSA and PMA. A relatively small weight decrease (ca. 5%) was observed well below 100 °C. The relevant relative maximum in the first derivative curve is in the 50–70 °C range, not far from the boiling point of methanol. The TGA curve of PMA shows a single further weight loss between 320 and 500 °C; the relevant maximum in the first derivative curve is observed at ca. 380 °C. This weight loss is almost complete and is attributed to the extensive de-polymerization of the polymer framework [15]. The same feature is apparent also in the TGA curve of PSA and the relevant maximum in the first derivative curve is practically coincident with that observed for PMA. This reflects the basically similar chemical structure of both CFAPs, which are mostly made of the same main co-monomer, DMAA. However, for PSA the main weight loss is preceded by a smaller (ca. 10%), pretty sharp one, in the 260–310 °C range. As the chemical structures of PSA and PMA differ only for the nature of the functional groups, we argue that this thermal event can be attributed to loss of sulfonic groups of PSA.

Inverse Steric Exclusion Chromatography (ISEC) was used to assess the nanometer scale morphology of water-swollen PSA, PMA and PVIP [16]. This is the working state of CFAPs during metalation and reduction. ISEC provides detailed information on the swollen-state morphology of cross-linked polymers. It is based on the analysis of elution volumes of solutes of known effective molecular size eluted through a chromatographic column where the material to be investigated is the stationary phase. Before loading the stationary phase into the column, it is swollen in the same solvent used as the mobile phase, so that the chromatographic behaviour depends on its morphology in the swollen state. Under proper conditions, partition of solutes between the mobile and stationary phase is influenced only by steric (entropic) effects and a simple geometrical model, such as Ogston's model (OM) can be applied [17]. OM depicts the pores within the swollen polymer framework (gel) as void spaces among randomly oriented rigid rods. When molecules of a solute are too big to enter the largest pore of the swollen gel, they are completely excluded from the stationary phase and their elution volume corresponds to *inter*particle volume only (dead volume). The difference between the volume of the chromatographic column (which is completely filled during the experiments) and the dead volume yields the true swollen-gel volume, which must be considered as an experimental value. Analysis of the chromatographic data based on OM provides a quantitative description of both the intensive parameters (polymer chain densities) and extensive properties (specific volumes of differently dense polymer fractions). This analysis is therefore best suited to compare quantitatively how easily molecular species can have access into swollen gels [12,15,18]. The mobile phase employed for the chromatographic runs was actually an aqueous 0.2 M Na_2SO_4 solution (the salts acts as a buffer of ionic strength [16c]), so that the CFAPs containing the sulfonic and carboxylic groups are in the Na^+ form (*vide infra*) during the analysis. The results of ISEC characterization

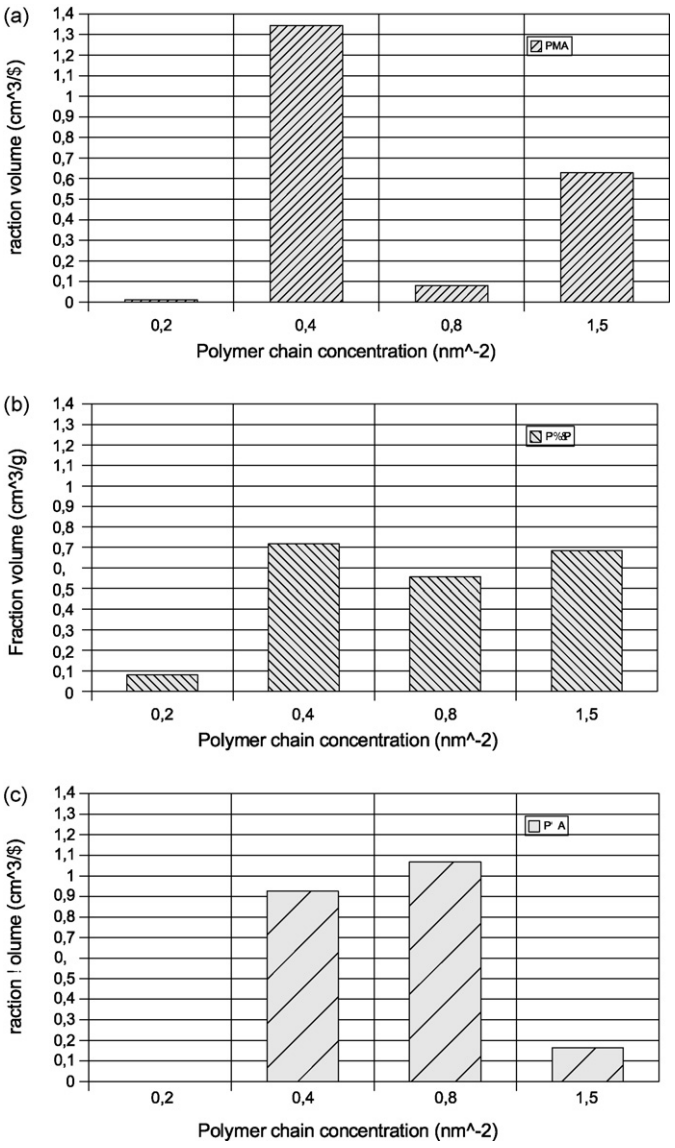

Fig. 1. Volume distribution of discrete fractions of polymer gel at different polymer chain concentrations in PSA (a), PMA (b) and PVIP (c) swollen with 0.2 M aqueous Na_2SO_4.

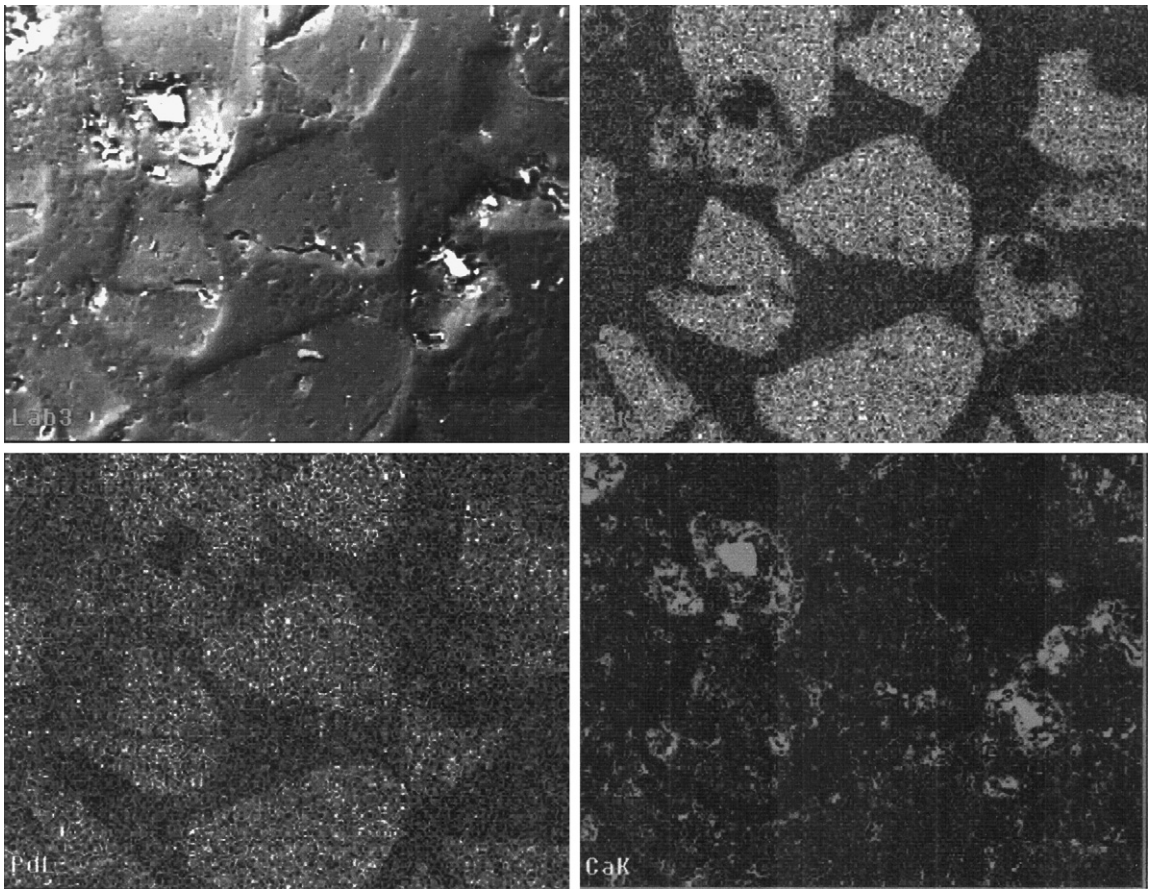

Fig. 2. XRMA scanning picture of a section of catalyst Pd^0/NaPSA, showing the sulfur (upper right) and palladium (lower left) distributions.

based on Ogston's model of the investigated CFAPs are illustrated in Fig. 1.

All the cross-linked polymers are gel-type [19] and have similar computed swollen-gel volumes. This reflects the circumstance that the most abundant co-monomer, DMAA, is the same for all of them, and swelling behaviour is accordingly similar. The computed swollen-gel volumes correspond to 90–96% of the experimental values. The agreement can be considered excellent and implies that essentially the whole swollen polymer framework was detected and only a negligible fraction of the material, if any, was too dense to exclude even the smallest chromatographic probes. PVIP has the largest proportion of the fraction with polymer chain concentration of 1.5 nm nm^{-3}. This is the most dense fraction for all the investigated CFAPs and is relatively poorly accessible. It is known that quite often pyridyl groups in polymers derived from vinylpyridine are poorly accessible, due to the formation of highly dense domains of the polymer framework [20]. The very low yield of metalation for PVIP (see below) indicates that most pyridyl groups are unavailable for metal co-ordination. The combination of these two arguments suggests that the pyridyl groups are concentrated in the most dense, hardly accessible fraction of the polymer framework. Also in PMA the fraction with polymer chain concentration of 1.5 nm nm^{-3} is relatively abundant and by analogy with PVIP it can be argued that the carboxylic groups within this domain of the polymer network will not be available for ion-exchange. By contrast, in PSA the fraction with polymer chain concentration of 1.5 nm nm^{-3} is negligible and a better accessibility of the polymer framework can be anticipated for this material.

3.2. Preparation and characterization (XRMA, low-resolution TEM) of Pd^0/CFAPs

The metalation of PSA and PMA was straightforward. Before the ion-exchange step, PMA was converted into the sodium form (NaPMA), by reaction with excess $NaBH_4$ in aqueous environment. This transformation increases its swelling degree in water and improves the accessibility of the polymer framework during the ion-exchange reaction.

The resins were treated with $[Pd(NH_3)_4](NO_3)_2$, which can undergo both ion-exchange (PSA) or metal co-ordination (PMA, PVIP). For PSA the metal uptake from water solutions, calculated with respect to the amount of metal complex, was quantitative

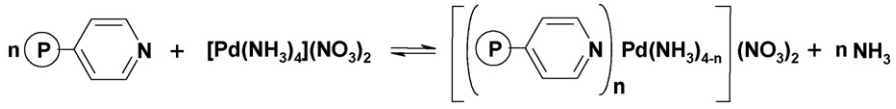

Scheme 4. Metalation of PVIP with palladium(II).

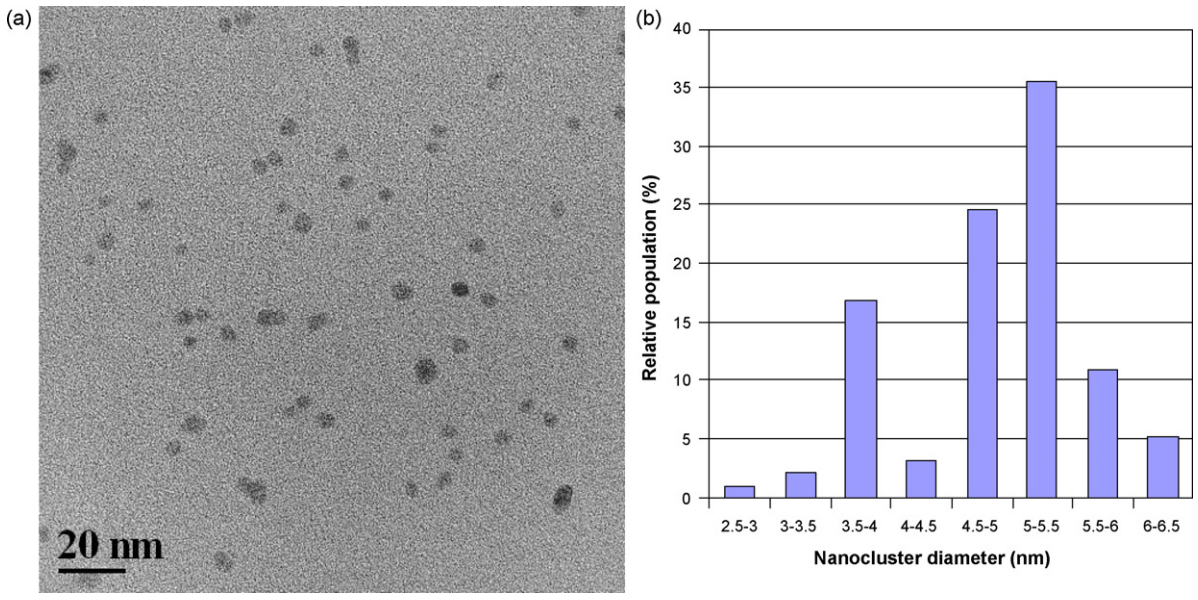

Fig. 3. Low-resolution TEM micrograph (a) and nanoclusters size distribution (b) of Pd^0/NaPSA (191 counts).

(98%), but in the case of NaPMA it was high, but not complete (87%). For PSA the initial Pd^{II}:SO_3H ratio was 1:4, corresponding to a final metal load of 1% (w/w) in the catalyst. For NaPMA, the Pd^{II}:CO_2Na ratio was 1:2, corresponding to a final metal load of 2% (w/w) in the catalyst. The higher amount of palladium employed per unit amount of functional groups and the likely unavailability of a fraction of the carboxylate groups for the ion-exchange reaction explain why the metal uptake for NaPMA, albeit high, was not complete.

When the metalated CFAPs were treated with excess $NaBH_4$ in aqueous environment, Pd^{II} was transformed into Pd^0 nanoclusters. As BH_4^- reduces also H^+ ions to H_2 and was used in excess, PSA was converted into its sodium form during the reduction step. The Pd^0 nanoclusters within the polymer framework of NaPSA were found to be evenly distributed (*vide infra*) (Fig. 2).

For PVIP the metal uptake was only 23% with respect to the initial amount of $[Pd(NH_3)_4](NO_3)_2$, which corresponds to a 1:2 Pd^{II}:pyr molar ratio. It is theoretically possible that all the co-ordinated ammonia molecules are displaced by the pyridyl groups of PVIP during the metalation (Scheme 4). With a 1:2 Pd^{II}:pyr starting molar ratio, this would correspond to full engagement of the functional groups in metal co-ordination and the uptake of only 50% of available metal.

In our case the observed value (23%) is even lower. This suggests that at least half pyridyl groups are not accessible to the metal complex and not available for the metalation, as anticipated in the discussion of ISEC characterization of the support.

Figs. 3–5 show the low-resolution TEM images of Pd^0/NaPSA, Pd^0/NaPMA and Pd^0/PVIP and the respective diameter distributions. Pd^0/NaPSA and Pd^0/PVIP exhibit similar size distribution hystograms, with the highest frequency around 5 nm. The size distribution of Pd^0/NaPMA is much wider than the other two. We can only speculate on the different size distributions of these catalysts.

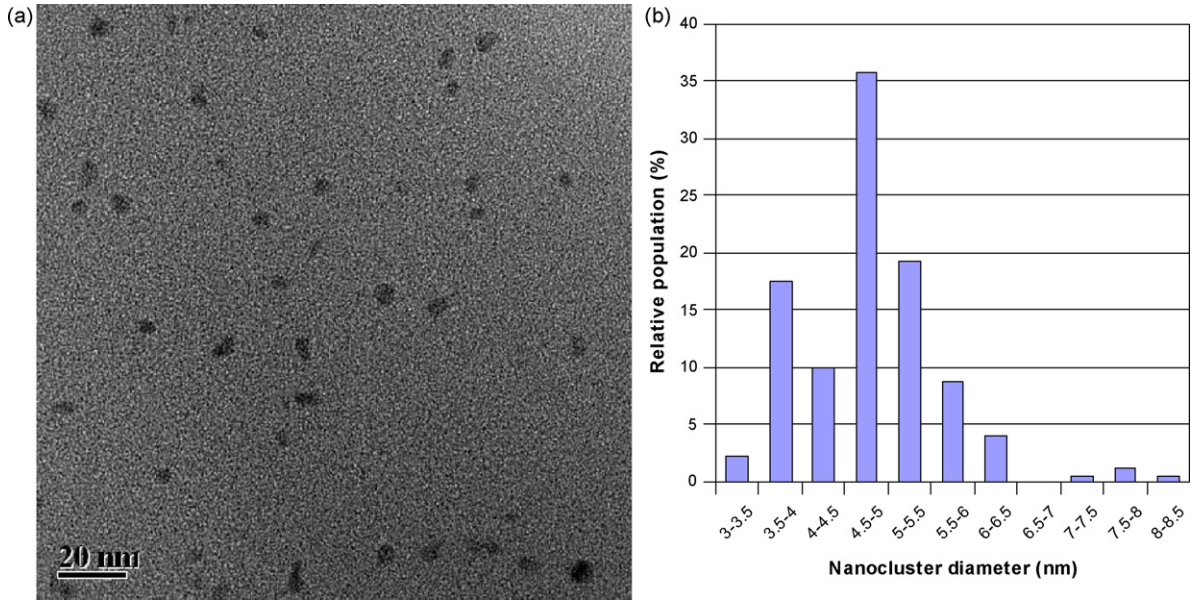

Fig. 4. Low-resolution TEM micrograph (a) and nanoclusters size distribution (b) of Pd^0/PVIP (172 counts).

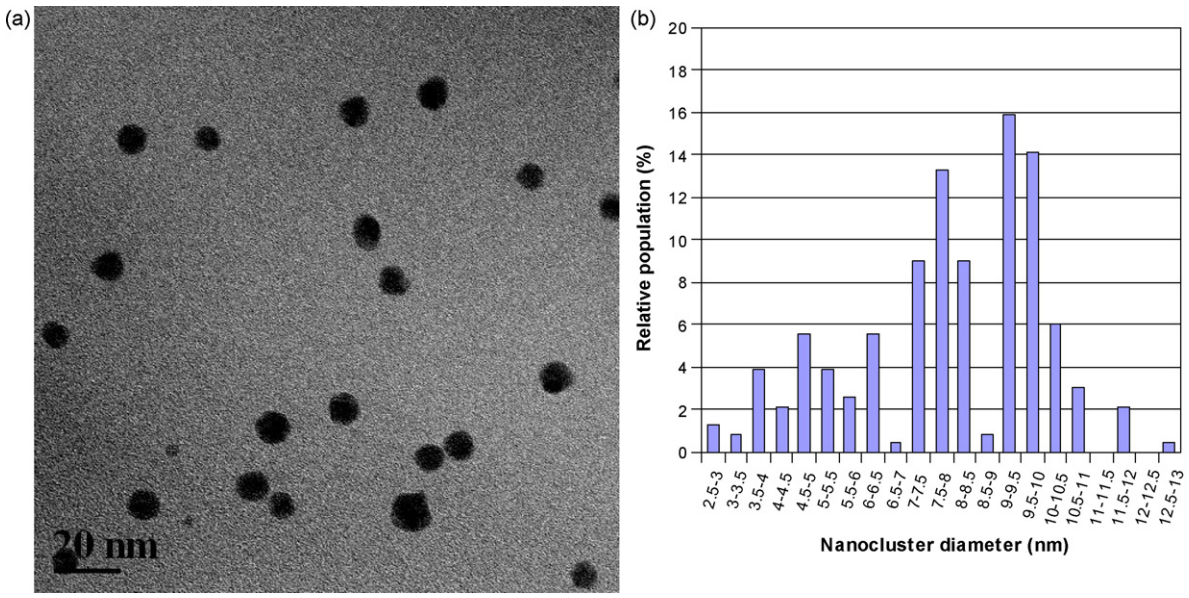

Fig. 5. Low-resolution TEM micrograph (a) and nanoclusters size distribution (b) of Pd^0/NaPMA (233 counts).

On one hand, functional groups could be responsible of the size control, if any [21]. On the other hand it is also known that the polymer chains can limit the size of metal [6,22,23] or metal oxide [24] nanoparticles growing within a polymer framework. The latter effect ("Template Controlled Synthesis", [6]) can be proved by crossing of the TEM and ISEC data. For our new catalysts this comparison is not conclusive and further investigation is necessary in this connection.

3.3. Catalysis: hydrogenation of alkenes

We have recently published a preliminary study on the performance of a Pd^0/CFAP catalyst, based on an acrylonitrile copolymer, in the hydrogenation of cyclohexene as compared to Pd^0/EnCat 30NP and Pd^0/Al_2O_3 [13b] and found that its activity was comparable, but lower, than both benchmark catalysts. However, tests of activity in solution after the separation of the solid catalysts showed that it was more stable than Pd^0/EnCat 30NP.

The investigation has been now extended to other catalysts (Pd^0/NaPSA, Pd^0/NaPMA, Pd^0/PVIP) and other hydrogenation reactions. The activity of the new catalysts was first screened in the hydrogenation of a model substrate such as cyclohexene, in methanol at 25 °C and 0.55 MPa. The kinetic plots for Pd^0/NaPSA, Pd^0/NaPMA and Pd^0/PVIP are illustrated in Fig. 6. As the hydrogen pressure was kept constant, the reaction is pseudo-zero order in H_2

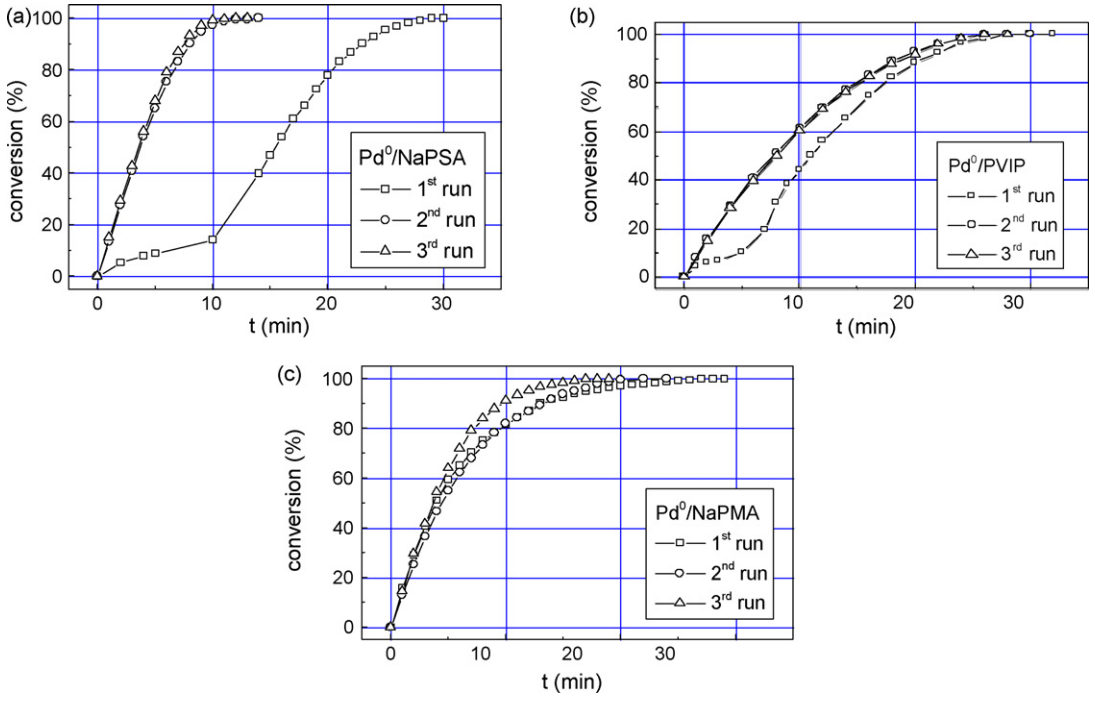

Fig. 6. Kinetic plots of the hydrogenation of cyclohexene (1 M, MeOH, 25 °C, 0.55 MPa) over Pd^0/NaPSA (a), Pd^0/PVIP (b), Pd^0/NaPMA (c).

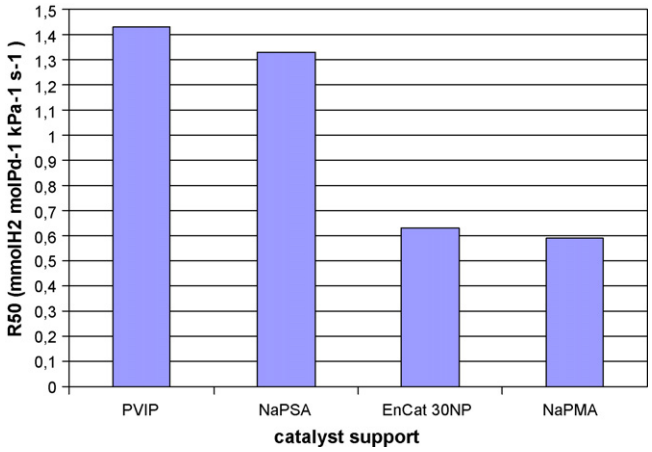

Fig. 7. Average reaction rates of cyclohexene hydrogenation at 50% conversion (R_{50}) in the second catalytic runs, calculated as mmol of H_2 consumed at 50% conversion per unit time (s), unit palladium amount (mol) and unit hydrogen pressure (kPa).

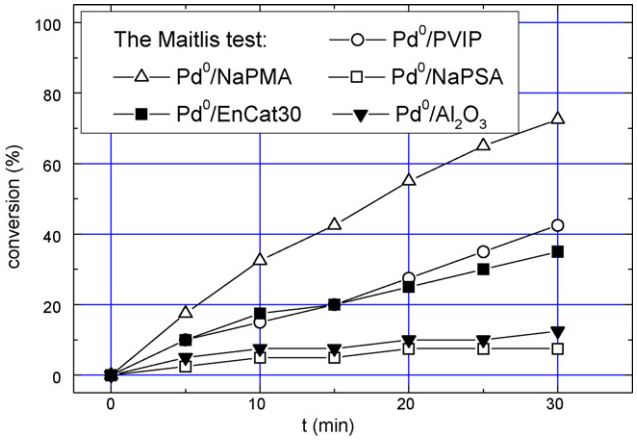

Fig. 8. Catalytic activity in the liquid phase after the first run of cyclohexene hydrogenation after the separation of the solid catalysts.

and the gas uptake actually corresponds to the alkene consumption rate.

The plots in Fig. 6 show that the catalysts have different behaviours during their respective first catalytic runs. Whereas Pd^0/NaPMA is immediately active, an induction period was observed in Pd^0/EnCat 30NP [13b]. We have found clear evidence of the presence of palladium acetate in Pd^0/EnCat 30NP [11b]. Palladium acetate is the precursor of metal nanoclusters in this catalyst and it seems likely that the induction period is due to the reduction of the residual amounts of the precursor, rather than palladium reoxidation upon standing in air. The behaviour of Pd^0/NaPSA and Pd^0/PVIP in the first run is somewhat different. In these cases, there is an initial period of immediate, relatively small activity. This declines within a few minutes, after which the catalysts turn out to be fully activated. This could be due to the presence of more than one active species in the fresh catalyst. However, all the catalysts could be recycled and in no induction time or initially low activity were observed in recycles. Additionally after being fully activated the catalysts show a stable performance for at least two further catalytic runs, which suggests that a single active phase is eventually generated.

For Pd^0/PMA there are very small differences in the plots of the three consecutive runs, but it is definitely slightly more active in the third run. For the other catalysts, the curves of the respective second and third runs are parallel to one another and almost parallel to the parts of the respective first run plots corresponding to the fully activated catalyst. Therefore, the performance of the catalysts in their second run is particularly representative and useful for comparative purposes. Average reaction rates per mole of palladium in the second runs at 50% conversion, normalized for the hydrogen pressure (R_{50}), are reported in Fig. 7. The value for Pd^0/EnCat 30NP from ref. [13b] is also included for comparative purposes.

Interestingly, the new Pd^0/CFAP catalysts are as active as (Pd^0/NaPMA) or considerably more active than (Pd^0/PVIP, Pd^0/NaPSA) Pd^0/EnCat 30NP. Whereas Pd^0/PVIP and Pd^0/NaPSA have similar nanocluster size (4.8 nm on average), Pd^0/NaPMA has much larger Pd^0 nanoclusters. As R_{50} goes in the order Pd^0/PVIP > Pd^0/NaPSA $\gg$ Pd^0/NaPMA it seems that the increase of nanocluster size somehow affects the specific hydrogenation rate and that in addition these values are affected by the diffusion. In the case of Pd^0/EnCat 30NP the size of palladium crystallites is even lower than in Pd^0/NaPSA and Pd^0/PVIP catalysts [10,11a]. In spite of this, the specific rate is as low as observed with Pd^0/NaPMA and this suggests that the EnCat catalyst exhibits the strongest diffusion limitations.

All the catalysts are quite stable and their activity does not decrease along the first three catalytic runs and in the case of Pd^0/NaPMA a small, but appreciable, increase in the catalytic activity is observed. To investigate on the stability of the catalysts under duty, we checked for activity in the liquid phase recovered after the first runs carried out with fresh catalyst samples. At the end of the reaction the catalyst was separated simply by decantation. The clear solutions obtained were then added with the substrated and the reaction was repeated in the absence of the solid catalyst. The results of these tests are illustrated in Fig. 8. The data for Pd^0/EnCat 30NP from ref. [11b] are also included for comparative purposes.

The observed activity in the liquid phase after the separation of the solid was remarkable for Pd^0/NaPMA, appreciable for Pd^0/PVIP and almost negligible for Pd^0/NaPSA. The latter catalyst is therefore quite stable and, apparently, its stability is much better than that of Pd^0/EnCat 30NP [13b], which is comparable with Pd^0/PVIP. It should be however appreciated that the activity left in the liquid phase is much lower than that observed in the presence of the solid materials. Therefore the solids are responsible for most of the observed catalytic activity (actually almost completely in the case of Pd^0/NaPSA).

The most straightforward explanation of activity in the liquid phase is metal leaching [25–27]. However, metal leaching is expected to lower the activity in recycled catalysts. Our catalysts did not show any reduction of activity. This is not enough to rule

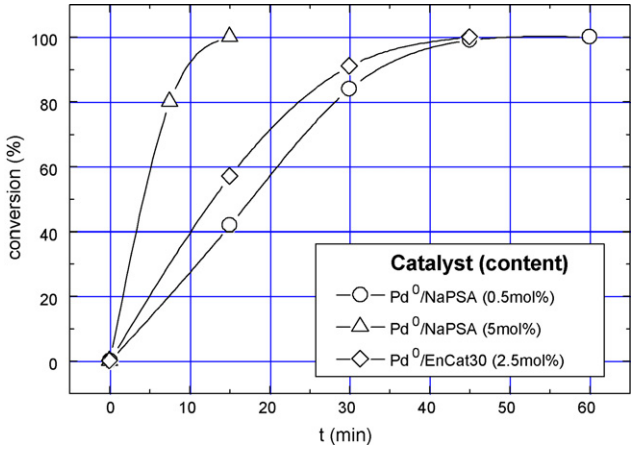

Fig. 9. Conversion (GC) *versus* time plots of the hydrogenation of *trans*-methylcinnamate (0.1 M, MeOH, room temperature, atmospheric pressure) over Pd^0/NaPSA and Pd^0/EnCat 30NP. [Courtesy of Reaxa Ltd., Manchester, UK].

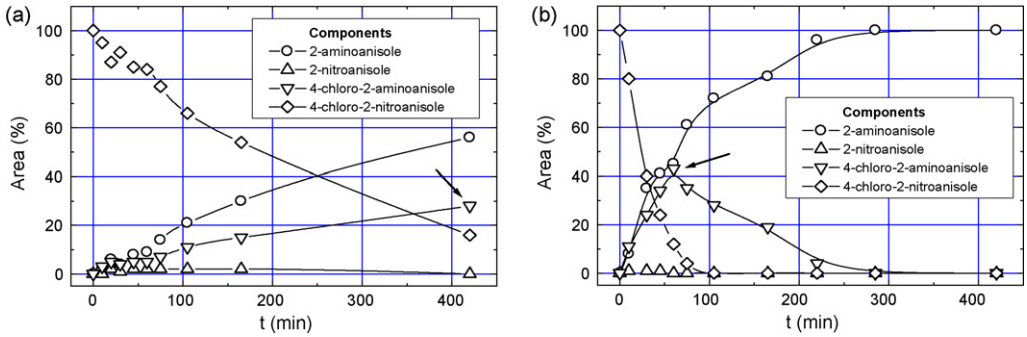

Fig. 10. Hydrogenation of 4-chloro-2-nitroanisole (0.1 M in methanol, room temperature, atmospheric pressure) over Pd^0/EnCat 30NP (a) and Pd^0Na/PSA (b) (Pd/nitroaromatic = 1/100, mol/mol). The arrow indicates the maximum observed yield of 4-chloro-2-aminoanisole (raw chromatographic areas). [Courtesy of Reaxa Ltd., Manchester, UK].

out metal leaching, but in the third run Pd^0/NaPMA, which showed the highest activity left in the liquid phase, worst performance in the split test, was slightly, but clearly, more active than in the previous two runs. This circumstance (highest activity in the liquid phase in the absence of the catalyst combined with the increase of activity upon recycling) suggests that the cause of instability could be different from metal leaching.

As pointed out above, in the tests of activity in the liquid phase the catalysts were separated by decantation and in this way clear solutions were recovered. However, it is possible that some very small catalysts' particles, invisible to the naked eye, were produced by the slight mechanical degradation of the solid. Very small, invisible fines could have remained suspended in the liquid phase and could be responsible of the observed activity in the liquid phase after the separation of the solids. At the same time breaking up of the catalysts particles under duty makes the solid particles smaller and increases their specific surface area, which would explain the apparent increase of activity of solid Pd^0/NaPMA upon recycling. This would explain the apparently puzzling observation of the increase of activity upon recycling in the least stable catalyst. However the data available so far are not conclusive with respect to the mechanism with which activity in the liquid phase builds up (leaching or mechanical degradation) and this is subject for further investigation. In any case, whatever the underlying mechanism, these results show that our best catalyst, Pd^0/NaPSA, is quite stable and reusable in the hydrogenation of cyclohexene. As a matter of fact it seems to be more stable than the commercially available Pd^0/EnCat 30NP.

Pd^0/NaPSA performed well also in the hydrogenation of *trans*-methylcinnamate. The relevant kinetic plots are illustrated in Fig. 9 and show that with Pd^0/EnCat 30NP a five-fold greater amount of active metal (Pd/substrate = 1/40, mol/mol) was required to achieve an apparent rate approaching the rate observed over Pd^0/NaPSA (Pd/substrate = 1/200, mol/mol).

The reaction likely proceeded under diffusion-controlled conditions: a ten-fold increase of the amount Pd^0/NaPSA (Pd/substrate ratio 1/20) made approximately the apparent rate to increase only twice. Therefore the different apparent rates observed over Pd^0/NaPSA and Pd^0/EnCat 30NP are likely due to much more effective diffusion limitation in the EnCat catalyst, in agreement with the results of cyclohexene hydrogenation. This would explain why Pd^0/EnCat 30NP was unable to surpass, or at least, equal the performance of Pd^0/NaPSA in spite of its small nanocluster size.

3.4. Catalysis: hydrogenation of 4-chloro-2-nitroanisole

The hydrogenation of 4-chloro-2-nitroanisole is a more challenging reaction, because the hydrodechlorination reaction can occur along with the hydrogenation of the nitro group into an amine group. Thus at least partial conversion of the substrate into 2-aminoanisole can be anticipated in our case. For this reason, palladium catalysts are not the catalysts of choice for selective hydrogenation of halo-nitroaromatics into the corresponding haloanilines. Nonetheless, this reaction is a model useful for comparative purposes. Fig. 10 shows its progress over Pd^0/EnCat 0NP and Pd^0Na/PSA (Pd/nitroaromatic = 1/100, mol/mol for both catalysts) at room temperature and atmospheric pressure, with the relative distribution of products and starting materials over time.

The curves cannot be used for fully quantitative comparison, because raw relative chromatographic areas are represented. In spite of this, they are highly informative on the different apparent activity and selectivity of the two catalysts. Again Pd^0/NaPSA was observed to catalyze the reaction significantly faster than Pd^0/EnCat 30NP. Whereas the substrate was not completely consumed over Pd^0/EnCat 30NP after 7 h, its complete conversion took less than 2 h over Pd^0/NaPSA. In addition, Pd^0/NaPSA is much more selective towards 4-chloro-2-aminoanisole. Whereas with Pd^0/EnCat 30NP the areas of 2-aminoanisole and 4-chloro-2-aminoanisole are always close to the 2/1 ratio, they are always practically the same in the first 60 min of reaction, i.e. up to almost complete conversion of the substrate. Only when 4-chloro-2-nitroanisole disappears 4-chloro-2-aminoanisole can be completely hydrodechlorinated to 2-aminoanisole.

4. Conclusions

Three Pd^0 heterogeneous catalysts were prepared using cross-linked, gel-type, functional acrylic polymers as the supports. The supports (PSA, PMA and PVIP) were easily obtained by quantitative co-polymerization of *N*,*N*-dimethylacrylamide with 2-acrylamido-2-methylpropane sulfonic acid, methacrylic acid or 4-vinylpyridine, respectively, in the presence of ethylene glycoldimethacrylate as the cross-linker. The Pd^0 catalysts (Pd^0/NaPSA, Pd^0/NaPMA, Pd^0/PVIP) were readily prepared treating the supports with aqueous solutions of $[Pd(NH_3)_4](NO_3)_2$ and reducing the metalated solids with $NaBH_4$ in an alcoholic solution. The performance of these catalysts was compared with that of commercial Pd^0/EnCat 30NP in the model hydrogenation of cyclohexene in methanol at 0.55 MPa. Pd^0/NaPSA and Pd^0/PVIP are more active than Pd^0/EnCat 30NP and Pd^0/NaPMA is almost as active. The performance of Pd^0/EnCat 30NP and of Pd^0/NaPMA was likely unfavourably affected by mass-transport restrictions. Follow-up of the reaction in the liquid phase after the separation of the solid catalyst showed some catalytic activity in the liquid phase. It is not clear at this stage whether this pertains to chemical or to mechanical instability of the catalysts, but Pd^0/NaPSA turned out to be very stable and, in any case, much more stable than Pd^0/EnCat 30NP.

Its performance was further compared with that of Pd^0/EnCat 30NP in the hydrogenation of *trans*-methylcinnamate and 4-chloro-2-nitroanisole, again taken as model reactions. Also in these additional tests Pd^0/NaPSA was much more active than Reaxa's catalyst. Not surprisingly, in the hydrogenation of 4-chloro-2-nitroanisole the main reaction was the hydrodechlorination over both catalysts, but remarkably in addition to higher activity a clearly higher selectivity towards the chlorinated aromatic amine was achieved too over Pd^0/NaPSA.

In conclusion, the preliminary tests described in this paper show that at least some Pd^0 catalysts supported on cross-linked, gel-type, functional acrylic polymers, prepared along a simple procedure we have been using since long, can be as attractive as the polyurea-supported catalysts already commercially available and should be taken into account for further development and optimization for technical applications.

Acknowledgments

We are grateful to Reaxa Ltd. (Manchester, UK) for loaning samples of EnCat materials. Dr. G. Pace (Istituto di Scienze e Tecnologie Molecolari, CNR – Padova), Mrs. Anna Moresco (Istituto di Chimica Inorganica e delle Superfici, CNR – Padova), Dr. Leonardo Tauro (Dipartimento di Geoscienze, Università di Padova) and Dr. Paolo Guerriero (Istituto di Chimica Inorganica e delle Superfici, CNR – Padova) are gratefully acknowledged for thermogravimetric, elemental, XRMA samples preparation and XRMA analysis, respectively.

References

[1] (a) M. Kralik, A. Biffis, J. Mol. Catal. A: Chem. 177 (2001) 113;
(b) B. Corain, M. Zecca, K. Jerabek, J. Mol. Catal. A: Chem. 117 (2001) 3.
[2] (a) M. Guisnet, J. Barrault, C. Bouchoule, D. Duprez, C. Montassier, G. Pérot (Eds.), Heterogeneous Catalysis and Fine Chemicals, Elsevier, Amsterdam, 1988;
(b) R.A. Sheldon, H. van Bekkum (Eds.), Fine Chemicals through Heterogeneous Catalysis, Wiley-VCH, Weinheim, 2001.
[3] J.M. Tibbitt, B.C. Gates, J.R. Katzer, J. Catal. 38 (1975) 505.
[4] P. Hodge, Chem. Soc. Rev. 26 (1997) 417.
[5] (a) J. Wöllner, W. Neier, German Patent 1193931, Bergbau und Chemie Homberg, Germany (1963);
(b) H. Giering, German Patent 1238453, Bergbau und Chemie, Homberg, Germany (1965);
(c) J. Wöllner, W. Neier, German Patent 1260454, Bergbau und Chemie, Homberg, Germany (1966);
(d) K. Weissermel, H. Arpe, Industrial Organic Chemistry, fourth ed., Wiley-VCH, Weinheim, 2003.
[6] B. Corain, K. Jeràbek, P. Centomo, P. Canton, Angew. Chem. Int. Ed. 43 (2004) 959.
[7] M. Zecca, P. Centomo, B. Corain, in: B. Corain, G. Schmid, N. Toshima (Eds.), Metal Nanoclusters in Catalysis and Materials Science: The Issue of Size Control, Elsevier, Amsterdam, 2008 (ISBN-13: 978-0-444-53057-8).
[8] T. Seki, J.-D. Grundwaldt, N. van Vegten, A. Baiker, Adv. Synth. Catal. 350 (2008) 691.
[9] (a) M.C. Wissler, U.-P. Jagush, B. Sundermann, W.F. Hölderich, Catal. Today 121 (2007) 6;
(b) W. Laufer, J.P.M. Niederer, W.F. Hölderich, Adv. Synth. Catal. 344 (2002) 1084.
[10] D. Pears, S.C. Smith, Aldrichim. Acta 38 (2005) 23.
[11] (a) C. Bolfa, A. Zoleo, A.S. Sassi, A.L. Maniero, D. Pears, K. Jerabek, B. Corain, J. Mol. Catal. A: Chem. 275 (2007) 233;
(b) P. Centomo, M. Zecca, B. Corain, A. Zoleo, A.L. Maniero, D.A. Pears, P. Canton, K. Jeřábek, Phys. Chem., Chem. Phys., submitted for publication.
[12] (a) A. Biffis, B. Corain, M. Zecca, C. Corvaja, K. Jeřábek, J. Am. Chem. Soc. 117 (1995) 1603;
(b) M. Zecca, A. Biffis, G. Palma, C. Corvaja, S. Lora, K. Jerabek, B. Corain, Macromolecules 29 (1996) 4655;
(c) A.A. D'Archivio, L. Galantini, A. Panatta, E. Tettamanti, B. Corain, J. Phys. Chem. B 102 (1998) 6774.
[13] (a) M. Zecca, R. Fisera, G. Palma, S. Lora, M. Hronec, M. Kralik, Chem. Eur. J. 6 (2000) 1980;
(b) L. De Zan, D. Gasparovicova, M. Kralik, P. Centomo, M. Carraro, S. Campestrini, K. Jerabek, B. Corain, J. Mol. Catal. A: Chem. 265 (2007) 1.
[14] B. Corain, P. Centomo, S. Lora, M. Kralik, J. Mol. Catal. A: Chem. 204–205 (2003) 755.
[15] F. Pozzar, A. Sassi, G. Pace, S. Lora, A.A. D'Archivio, K. Jeràbek, A. Grassi, B. Corain, Chem. Eur. J. 11 (2005) 7395.
[16] (a) K. Jeràbek, Anal. Chem. 57 (1985) 1595;
(b) K. Jeràbek, Anal. Chem. 57 (1985) 1598;
(c) K. Jeràbek, in: M. Potschka, P.L. Dubin (Eds.), Cross Evaluation of Strategies in Size-Exclusion Chromatography, ACS Symposium Series 635, American Chemical Society, Washington DC, USA, 1996, p. 211.
[17] A.G. Ogston, Trans. Faraday Soc. 54 (1958) 1754.
[18] K. Jeràbek, J. Mol. Catal. 55 (1989) 247.
[19] A. Guyot, in: D.C. Sherrington, P. Hodge (Eds.), Synthesis and Separations Using Functional Polymers, Wiley, New York, 1988, p. 1.
[20] K. Jerabek, H. Widdecke, B. Fleischer, React. Polym. 19 (1993) 81.
[21] R.G. Finke, S. Özkar, Coord. Chem. Rev. 248 (2004) 135.
[22] S.N. Sidorov, L.M. Bronstein, V.A. Davankov, M.P. Tsyurupa, S.P. Solodovnikov, P.M. Valetsky, Chem. Mater. 11 (1999) 3210.
[23] C. Burato, P. Centomo, G. Pace, M. Favaro, L. Prati, B. Corain, J. Mol. Catal. A: Chem. 238 (2005) 26.
[24] R.F. Ziolo, E.P. Giannelis, B.A. Weinstein, M.P. O'Horo, B.N. Ganguly, V. Mehrotra, M.W. Russell, D.R. Huffman, Science 257 (1992) 219.
[25] R.A. Sheldon, M. Wallau, I.W.C.E. Arends, U. Schuchardt, Acc. Chem. Res. 31 (1998) 485.
[26] J.A. Widegren, R.G. Finke, J. Mol. Catal. A: Chem. 198 (2003) 317.
[27] A. Biffis, M. Zecca, M. Basato, J. Mol. Catal. A: Chem. 173 (2001) 249.